LIPOPOLYSACCHARIDE DISRUPTS MITOCHONDRIAL PHYSIOLOGY IN SKELETAL MUSCLE VIA DISPARATE EFFECTS ON SPHINGOLIPID METABOLISM

Melissa E. Hansen, Kurtis J. Simmons, Trevor S. Tippetts, Mikayla O. Thatcher, Rex R. Saito, Sheryl T. Hubbard, Annie M. Trumbull, Brian A. Parker, Oliver J. Taylor and Benjamin T. Bikman

Department of Physiology and Developmental Biology, Brigham Young University, Provo, Utah

ABSTRACT—Lipopolysaccharides (LPS) are prevalent pathogenic molecules that are found within tissues and blood. Elevated circulating LPS is a feature of obesity and sepsis, both of which are associated with mitochondrial abnormalities that are key pathological features of LPS excess. However, the mechanism of LPS-induced mitochondrial alterations remains poorly understood. Herein we demonstrate the necessity of sphingolipid accrual in mediating altered mitochondrial physiology in skeletal muscle following LPS exposure. In particular, we found LPS elicited disparate effects on the sphingolipids dihydroceramides (DhCer) and ceramides (Cer) in both cultured myotubes and in muscle of LPS-injected mice. Although LPS-treated myotubes had reduced DhCer and increased Cer as well as increased mitochondrial respiration, muscle from LPS-injected mice manifested a reverse trend, namely elevated DhCer, but reduced Cer as well as reduced mitochondrial respiration. In addition, we found that LPS treatment caused mitochondrial fission, likely via dynamin-related protein 1, and increased oxidative stress. However, inhibition of *de novo* sphingolipid biosynthesis via myriocin protected normal mitochondrial function in spite of LPS, but inhibition of DhCer desaturase 1, which increases DhCer, but not Cer, exacerbated mitochondrial respiration with LPS. In an attempt to reconcile the incongruent effects of LPS in isolated muscle cells and whole muscle tissue, we incubated myotubes with conditioned medium from treated macrophages. In contrast to direct myotube LPS treatment, conditioned medium from LPS-treated macrophages reduced myotube respiration, but this was again mitigated with sphingolipid inhibition. Thus, macrophage sphingolipid production appears to be necessary for LPS-induced mitochondrial alterations in skeletal muscle tissue.

KEYWORDS—Ceramides, dihydroceramides, mitochondrial dynamics, respiration

INTRODUCTION

Metabolic and immune functions are crucial components of life. Once considered distinct, the remarkable eruption of evidence over the last 20 years not only indicates an interconnection between these two functions, but also reliance (1). Indeed, obesity, evidence of altered metabolic function, promotes the production of myriad immune mediators in adipocytes (2). Furthermore, we have long known that immune actions such as pathogen detection and resolution are highly energetic processes, eliciting changes in metabolic substrate and activity (3).

The mechanisms whereby immune actions alter metabolic actions either stem from characteristics of the pathogen itself or progress to the activation of a related receptor and subsequent downstream signaling. Lipopolysaccharide (LPS) is one example; LPS is a large molecule found on the surface of gram-negative bacteria and is regularly inhaled and ingested

(4). In recent years, a great degree of research has established that LPS, and activation of pattern-recognition receptors (5), is increased in states of metabolic disruption and, in fact, may be a primary cause of the altered metabolic state (6–8). This phenomenon is relevant in overt sepsis (9), but also decidedly metabolic alterations like obesity (10).

One potential mechanism whereby LPS may mediate metabolic disruption is its effect on sphingolipid metabolism. We previously found that activation of pattern-recognition receptors, like TLR4 or RAGE, which are activated with LPS, increases expression and activity of multiple biosynthetic enzymes and increases sphingolipid accrual, such as dihydroceramides (DhCer) and ceramides (Cer), in several tissues (11), which can subsequently alter metabolic function (8,12–14). Skeletal muscle is a mitochondria-rich and LPS-responsive tissue. Thus, given the necessity of healthy mitochondria on normal metabolic function, as well as the increasing frequency of obesity (15) and sepsis in clinical settings (16), elucidating the muscle mitochondrial effects of LPS may help improve our understanding of the mechanism of LPS-induced metabolic disruption. The purpose of this study was to determine both the effect of LPS on skeletal muscle mitochondrial function and the role of DhCer and Cer in mediating LPS-induced mitochondrial alterations.

MATERIALS AND METHODS

Animals

All experiments were performed on male C57Bl/6 mice between 18- and 20-wk old. Studies were conducted in accordance with the principles and procedures outlined in the National Institutes of Health Guide for the Care

and Use of Laboratory Animals and were approved by the Institutional Animal Care and Use Committee at Brigham Young University. All animals were housed in a temperature controlled ($20°C-21°C$) environment with a 12 h:12 h light–dark cycle. Water and food (Harlan Teklad; 8604) were administered *ad libitum*. Myriocin, a potent inhibitor of the rate-limiting enzyme in ceramide biosynthesis, serine palmitoyltransferase, was delivered via intraperitoneal injections three times per week at a dosage of 0.3 mg/kg. Mice in LPS treatment groups received daily intraperitoneal injections of LPS at a dosage of 1 mg/kg for a period of 28 d. Doses of both compounds were based on established use (12,14).

Cell culture

C2C12 murine myoblasts (passage 8–12; ATCC) and RAW264.7 macrophages (passage 4–6; ATCC) were maintained in Dulbecco's Modified Eagle Medium (DMEM) plus 10% fetal bovine serum (Invitrogen). For differentiation into myotubes, C2C12 myoblasts were grown to confluency and the medium was replaced with DMEM plus 10% horse serum (Invitrogen). Myotubes were used for experiments on day 4 of differentiation. For LPS treatment, O55:B5 LPS from *Escherichia coli* (Sigma-Aldrich; L2880) was diluted in ddH_2O in a 1 mg/mL stock. For myriocin treatment, myriocin (Sigma-Aldrich; M1177) was diluted in methanol in a 5 mM stock solution. Conditioned medium was prepared by incubating macrophages in treatment conditions for 12 h, after which this macrophage medium was transferred to myotubes for 12 h. Culture medium LPS levels were assessed by following the manufacturer's recommendations with the Pierce LAL Chromogenic Endotoxin Quantitation Kit (8828).

Lipid analysis

For ceramide-specific lipid isolation, homogenized tissues were resuspended in 300 μL ice-cold phosphate-buffered saline (PBS) and 1.5 mL of methanol. Five hundred picomoles of internal C-17 ceramide (Avanti Lipids; 860647) standard were spiked into each sample. Samples were centrifuged and supernatant was transferred to a clean tube. Following the addition of 30 μL of 1 M KOH in methanol, samples were incubated overnight at°C. Samples were dried to 50% volume and 25 μL glacial acetic acid was added to neutralize KOH. Separation of aqueous and organic phases required addition of 300 μL LC-grade chloroform and 600 μL DDH2O followed by centrifugation for 2 min at maximum speed. The lower organic phase was transferred to a fresh vial. This separation step was repeated twice. All lipid samples were dried in a vacuum centrifuge (Eppendorf Concentrator Plus). Analysis was performed as described previously (12).

Mitochondrial morphology

C2C12 myoblasts were grown to confluence in chamber slides (NUNC Lab-Tek II Chambered Coverglass System; 155382) and differentiated at day 4. The mitochondrial dye MitoTracker Red CMXRos (Molecular Probes; M7512), dissolved in anhydrous dimethylsulfoxide, was added to cultured myotubes at a concentration of 250 nM. The cells were incubated for 30 min at 37°C in the dark and then visualized using a confocal microscope (Olympus IX81). Following image capture, a blind assessment of mitochondrial morphology was performed and quantified. For muscle mitochondria imaging, gastrocnemius was extracted and fixated in 0.1 M sodium cacodylate and 3% gluteraldehyde at pH 7.3 for 3 h. The tissues were washed in 0.1 M sodium cacodylate ($6\times$, 10 min) and then washed in ddH_2O ($6\times$, 10 min). Postfixation occurred in 1% OsO_4 (0.1 M, 2 h, 22°C). The samples were then soaked overnight in 0.5% uranyl acetate at 4°C. The tissues were dehydrated in a graded series of acetone (10 min, 10%, 30%, 50%, 70%, 95%, 100%, $3\times$) and then embedded in Spurrs® resin. Ultrathin sections (90 nm thick) were cut with a microtome and diamond blade and then stained with 0.4% lead citrate. The samples were then imaged with transmission electron microscopy. Average diameter was determined by relative size of the standard (i.e., 1 μm) using Image J software.

Quantitative real-time PCR

Total RNA was extracted and purified from tissues using TRIzol (Invitrogen) according to the manufacturer's recommendations and as indicated previously (12,17,18). Briefly, cDNA was synthesized from mRNA via reverse-transcriptase PCR using a commercial cDNA synthesis kit with oligo(dT) primers (iScript Select cDNA Synthesis; Bio-Rad). Quantitative real-time PCR was performed with Evagreen Ssofast (Bio-Rad) using a BioRad CFX Connect Real-Time PCR Detection system. Primer sequences were 5′-ACAGGATG-CAGAAGGAGATTAC and 5′-CACAGAGTACTTGCGCTCAGGA as forward and reverse primers for actin, 5′-ACTTGACCTCCCTACTGGC and 5′-TCCTCTATCCCGTTGACACC as forward and reverse primers for *Drp-1*, and 5′-AAGTCCGGGAAGCTGAAAGT and 5′-TCTCGGTTATGGAAC-CAACC as forward and reverse primers for *Mfn2*. β-Actin reactions were

performed side by side with every sample analyzed. Changes in mRNA level of each gene for each treatment were normalized to that of the β-actin control mRNA according to Pfaffl (19).

Protein analysis

Tissue and cell extracts lysed and protein content was determined using a bicinchoninic acid protein assay (Pierce, Rockford, IL) and sample volumes were adjusted so that precisely 50 μg of protein was loaded into each lane. After addition of sample buffer, samples were resolved by SDS–PAGE, transferred to nitrocellulose, and immunoblotted using methods described previously (20). After incubation with primary antibody, blots were incubated with a horse-radish peroxidase-conjugated secondary antibody. Horseradish peroxidase activity was assessed with enhanced chemiluminescence solution (Thermo Scientific, Rockford, IL) and exposed to film. Primary antibodies: OxPhos Complex Kit (Invitrogen; 457999) and Actin (Cell Signaling; 8457S). Secondary antibodies: anti-mouse (Cell Signaling; 7076S) anti-rabbit (Cell Signaling; 7074S).

Cell and muscle fiber bundle permeabilization

For cells, C2C12 myotubes were detached in culture dishes with 0.05% trypsin-EDTA (Sigma) and growth medium was added to the culture. Contents were transferred to a tube and centrifuged for 10 min at 1,000 rpm at RT. After removal of supernatant, cells were resuspended in mitochondrial respiration buffer 05 (MiR05; 0.5 mM EGTA, 10 mM KH_2PO_4, 3 mM $MgCl_2$-6 H_2O, 60 mM K-lactobionate, 20 mM HEPES, 110 mM Sucrose, 1 mg/mL fatty acid free BSA, pH 7.1) plus 1 mg/mL digitonin and gently rocked at RT for 5 min before centrifugation at 1,000 rpm for 5 min. After discarding supernatant, cells were then suspended in 2.2 mL warm MiR05 and transferred to chambers in the O2K (Oroboros Instruments). Following respiration protocol (outlined below), cells were removed from the chambers and used for further analysis, including protein quantification. For skeletal muscle use, red gastrocnemius was quickly removed from mice and immediately placed in ice-cold MiR05 and trimmed of connective tissue. Small fiber bundles were prepared and gently separated along their longitudinal axis under a surgical scope (Olympus, ST) to a size of around 1 mg. Bundles were then transferred to a tube with chilled MiR05 and 50 μg/mL saponin and rocked at 4°C for 30 min, and then washed in MiR05 at 4°C for at least 15 min.

Mitochondrial respiration

High-resolution O_2 consumption was determined at 37°C in permeabilized cells and fiber bundles (MiR05) using the Oroboros O2K Oxygraph. Before addition of sample to respiration chambers, a baseline respiration rate was determined. After addition of sample, the chambers were hyperoxygenated to approximately 350 nmol/mL. Following this, respiration was determined according to various substrate–uncoupler–inhibitor–titration protocols. To determine general electron transport system function, electron flow through complex I was supported by glutamate + malate (GM; 10 and 2 mM, respectively, for cells) or GM + succinate (10 mM, for tissue) to determine oxygen consumption from proton leak (GM_L). Following stabilization, ADP (2.5 mM) was added to determine oxidative phosphorylation capacity (GM_P). The integrity of the outer mitochondrial membrane was then tested by adding cytochrome c (10 μM; not shown). Succinate was added (GMS_P; 10 mM, for cells) for complex I + II electron flow into the Q-junction. To determine full electron transport system capacity over oxidative phosphorylation, the chemical uncoupler carbonyl cyanide 4-(trifluoromethoxy) phenylhydrazone (FCCP) was added (0.05 μM, followed by 0.025 μM steps until maximal O2 flux was reached; GMS_E, for cells). Lastly, residual oxygen consumption was measured by adding antimycin A (2.5 μM) to block complex III action, effectively stopping any electron flow and providing a baseline respiration.

Intraperitoneal macrophage harvest

Intraperitoneal macrophages were harvested from LPS-injected mice as described previously (21).

Oxidative stress

Reactive oxygen species production was determined via incubation of cells with the radical-sensitive dichlorofluorescin (DCF). Briefly, following treatment, cells were washed with warm PBS, and then incubated in 50 μM DCF in 1% BSA (Invitrogen) in DMEM (Sigma). Following a 30-min incubation, cells were washed with PBS and then Krebs-Ringer Buffer was added. Fluorescence was measured using the excitation/emission wavelengths 485/530 nm with a Biotek microplate reader.

Statistics

Data are presented as the mean ± SEM. Data were compared by ANOVA with Tukey post hoc analysis (Graphpad Prism; La Jolla, CA). Significance was set at $P < 0.05$.

RESULTS

LPS increases Cer, mitochondrial respiration, and ROS generation in myotubes

Our initial aim was to confirm the effects of LPS treatment on ceramide accrual in murine myotubes. We found that Cer significantly increased in myotubes following an overnight LPS exposure (Fig. 1B) and that this was likely due to increased *de novo* biosynthesis considering the robust increase in expression of an isoform of the rate-limiting step in *de novo* ceramide synthesis, serine palmitoyltransferase (SPT) 1 (Fig. 1A). Based on our previous findings of ceramide reducing respiration (12,14,22), we anticipated this would lead to a reduction in mitochondrial respiration, but this was not the case. LPS treatment in myotubes significantly increased respiration, which remained elevated with addition of myriocin, a potent SPT inhibitor (Fig. 2A). Measurement of reactive oxygen species production via DCF fluorescence revealed that LPS alone increased oxidative stress in the cells (Fig. 2B), but not with ceramide biosynthesis inhibition via myriocin incubation. The increased ROS production with LPS may reveal an oxygen outlet explaining the increased mitochondrial respiration.

LPS increases complex IV and leads to mitochondrial fission in myotubes

Previous reports have found a temporal effect on decreasing and then increasing mitochondrial complex IV (23). We found
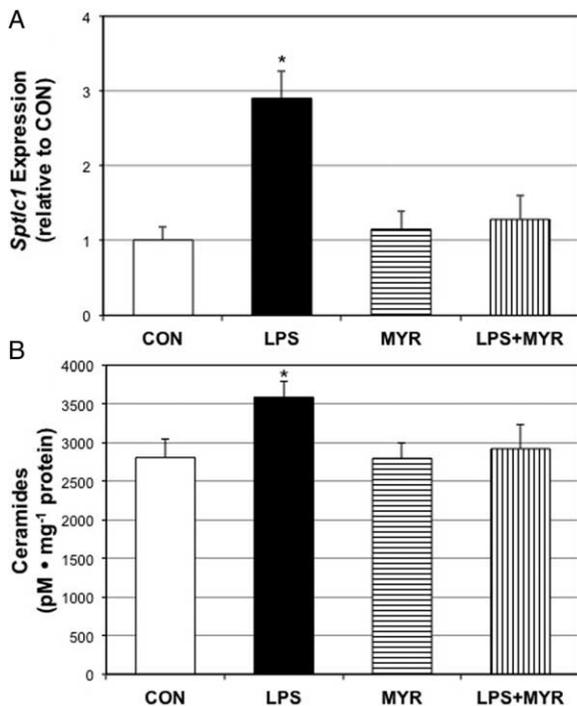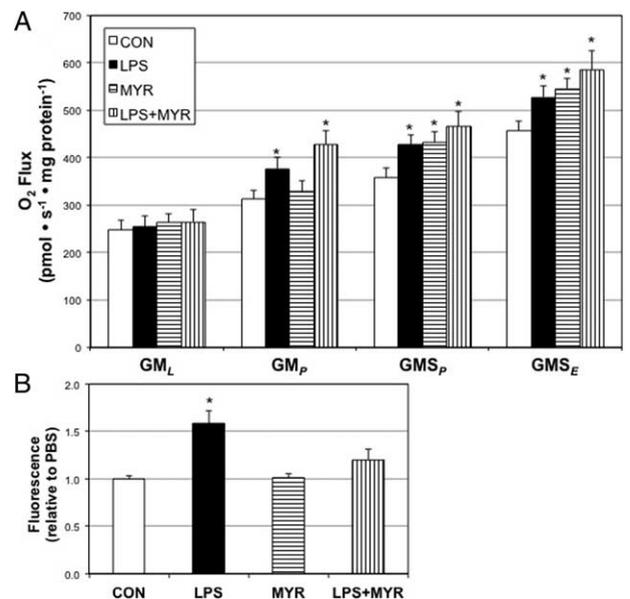
FIG. 2. **LPS increases mitochondrial respiration and ROS generation in C2C12 myotubes.** To measure mitochondrial respiration (A; n = 5), C2C12 myotubes were treated with LPS (100 ng/mL) ± myriocin (10 µM) for 12 h. GM_L indicates glutamate (10 mM) + malate (2 mM); GM_P +ADP (2.5 mM); GMS_P +succinate (10 mM); GMS_E, +FCCP (0.05 µM). DCF fluorescence was used to determine radical production (B; n = 5). *$P < 0.05$ for treatment versus CON.

that a 12-h incubation with LPS increased complex IV in myotubes (Fig. 3, A and B). Interestingly, this same treatment resulted in increased expression of dynamin-related protein 1 (DRP1), a gene whose product is involved in mediating mitochondrial fission (Fig. 3C), but did not affect proteins involved with fusion (e.g., mitofusin 1 and 2; data not shown). Indeed, we observed an apparent greater degree of segmented, distinct mitochondria with LPS treatment (Fig. 3, D and E), but not with myriocin cotreatment.

Chronic LPS injection increases skeletal muscle Cer, but not respiration, in mice

Following the 4-wk injection treatment, Cer were quantified in soleus muscle and found to be roughly 50% greater following LPS injection compared with vehicle (PBS; Fig. 4A). However, mice receiving concurrent myriocin injections had soleus ceramide levels comparable to control. In contrast to our findings in isolated myotubes, LPS treatment decreased mitochondrial respiration in red gastrocnemius (Fig. 4B). But once again, ceramide inhibition via myriocin restored respiration levels similar to control. Unlike myotubes, mitochondrial complex IV was diminished in gastrocnemius with LPS injections compared with other treatments (Fig. 5, A and B). However, gastrocnemius from LPS-injected mice had significantly smaller subsarcolemmal mitochondria compared with other treatments (Fig. 5, C and D).

Mitochondrial respiration is reduced in myotubes treated with macrophage-conditioned medium

To more closely replicate the *in vivo* milieu in an *in vitro* model, we treated macrophages with the same four treatments, i.e., CON, LPS, MYR, LPS + MYR, before transferring culture

FIG. 1. **LPS increases ceramides in C2C12 myotubes.** C2C12 myotubes were treated with LPS alone (100 ng/mL), myriocin alone (MYR; 10 µM), or myriocin with LPS (LPS + MYR) for 12 h. Following treatment, samples were used to quantify gene expression of *sptlc1* (A; n = 5) and ceramides via LCMS (B; n = 5). *$P < 0.05$ for LPS versus all other treatments.
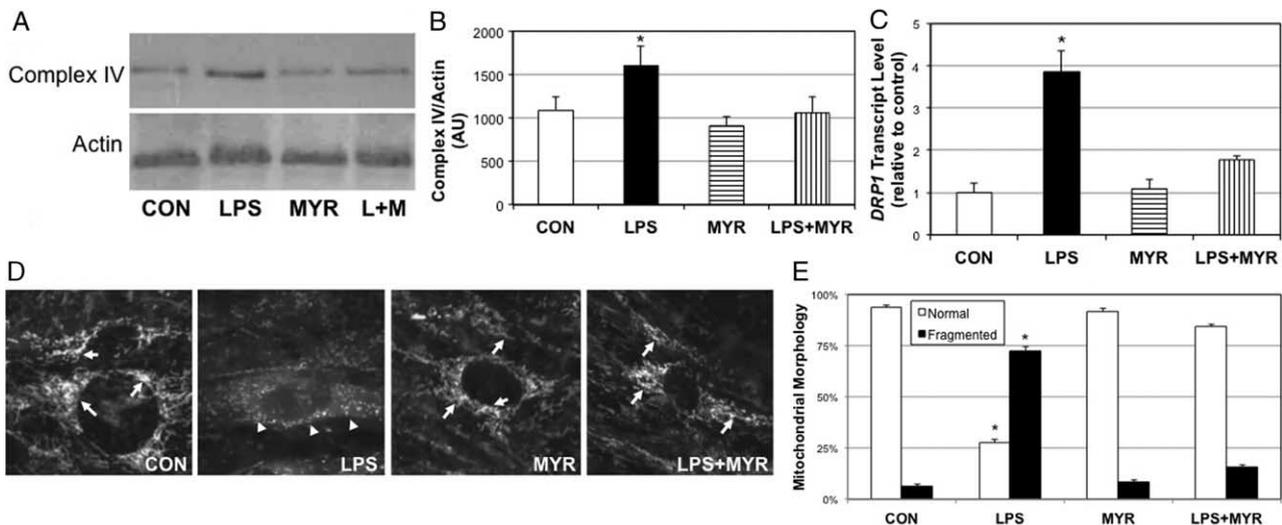
FIG. 3. **LPS increases mitochondrial complex IV and induces fission in C2C12 myotubes. Mitochondrial complex IV (A and B; n = 3) and DRP1 transcript expression (C; n = 5) were measured in C2C12 myotubes treated with LPS (100 ng/mL) $\pm$ myriocin (10 μM) for 12 h.** Cells were stained with Mitotracker Red following treatment and visualized via confocal microscopy (D; white arrows indicate sections of fusion, white arrowheads indicate fission; n = 3), followed by assessment of mitochondrial morphology (E; n = 3). $^*P < 0.05$ for treatment versus CON.

medium to myotubes. Cer were quantified in the macrophage culture medium in a subset of samples, which revealed a significant increase in both LPS-treated conditions, albeit diminished with myriocin addition compared with LPS alone (Fig. 6A). The conditioned medium elicited a similar effect on myotube lipid levels following incubation (Fig. 6B). This system allowed us to determine whether the macrophage is necessary for the disparate effects of LPS on muscle cell versus muscle tissue. We found that myotubes treated with conditioned medium from LPS-treated macrophages experienced a significant reduction in mitochondrial respiration (Fig. 6C), but not when macrophages were concurrently treated with myriocin. In contrast to direct LPS treatment, myotubes treated with conditioned medium from LPS-treated macrophages experienced only a slight, but significant increase in oxidative stress compared with CON alone (Fig. 6D). LPS levels in culture had no significant change over time and across conditioned medium exchange (Fig. 6E).

DhCer inversely correlate with LPS-induced mitochondrial disruption in skeletal muscle

In contrast to Cer, which were increased in all LPS-treated conditions (i.e., isolated cells and whole tissue) and thus not apparently directly responsible for the disparate alterations in mitochondrial physiology from cell to tissue, DhCer, the ceramide precursor, more closely followed the changes in mitochondrial respiration. In C2C12 myotubes, DhCer tended to be reduced with LPS treatment ($P = 0.054$) and were significantly reduced with myriocin addition (Fig. 7A). Myriocin inhibits the initial step of *de novo* ceramide biosynthesis, effectively reducing levels of both Cer and precursor DhCer. In contrast to our findings using myriocin, addition of fenretinide (FEN), an inhibitor of DhCer desaturase, resulted in an accrual of DhCer (Fig. 7A). Complex IV levels were markedly reduced in both FEN-treated conditions (Fig. 7, B and C). Mitochondrial respiration tended to change inversely with DhCer (Fig. 7D), where FEN-treated cells experienced the

lowest rates of respiration. We were unable to determine macrophage-secreted DhCer, as DhCer in conditioned medium from macrophages were essentially below reliable detection (data not shown). However, we found that DhCer were increased in the muscle of the LPS-treated mice following 4 wk of injection, but not with myriocin coinjection (Fig. 8).
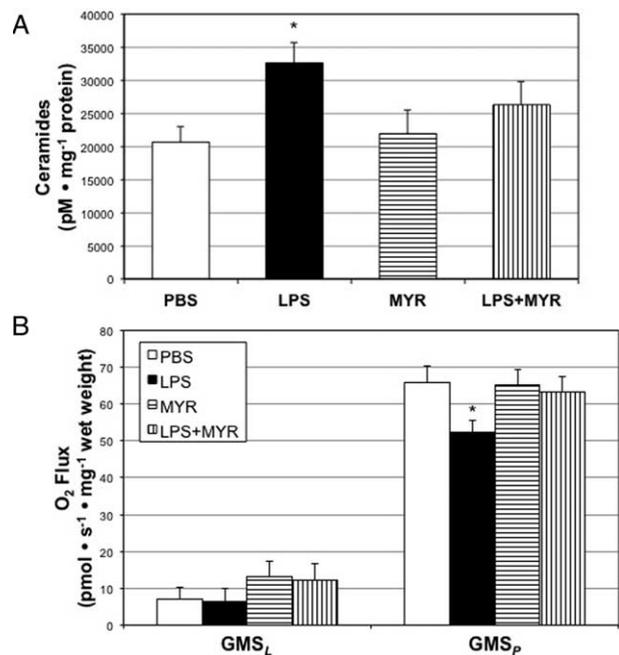

FIG. 4. **LPS injection increases skeletal muscle ceramides and reduces respiration in mice.** Adult male mice received IP injections of LPS (0.1 mg/kg body weight, daily) $\pm$ myriocin (0.3 mg/kg body weight, 3$\times$ per week) for 4 wk. Following treatment, soleus was excised and lipids extracted and quantified (A; n = 6). For respiration (B; n = 6), red gastrocnemius was excised, permeabilized, and treated with various substrates to measure mitochondrial respiration (see "Methods" for treatment details.) GMS$_L$ indicates glutamate (10 mM) + malate (2 mM) + succinate (10 mM); GMS$_P$ +ADP (2.5 mM). $^*P < 0.05$ for treatment versus PBS.
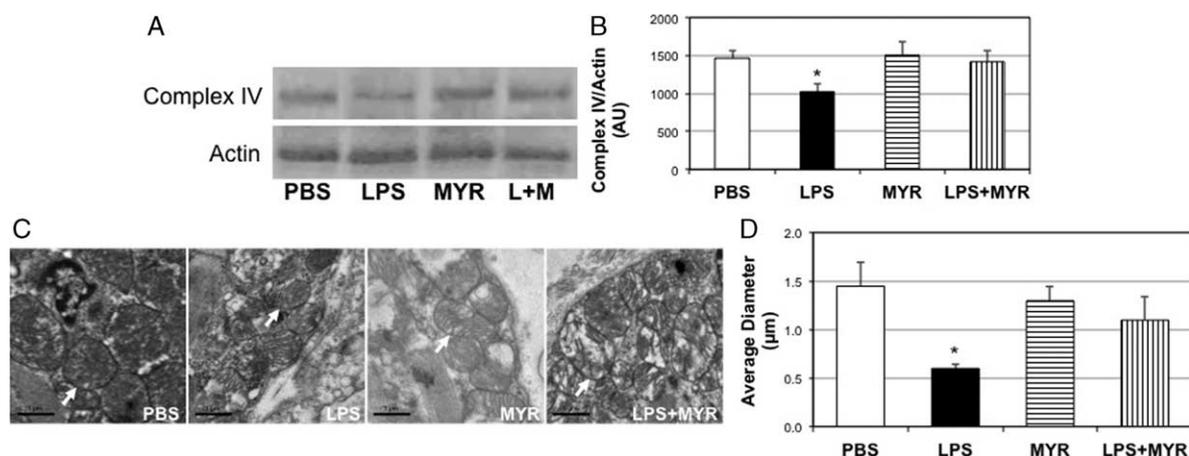
Fig. 5. **LPS injection may alter skeletal muscle mitochondrial morphology.** Adult male mice received IP injections of LPS (0.1 mg/kg body weight, daily) for 4 wk. Following treatment, complex IV protein was determined in gastrocnemius (A and B; n = 6). A portion of the gastrocnemius was used for imaging of mitochondria via EM (B; n = 3), with average greatest diameter quantified (C; n = 3). $^*P < 0.05$ for treatment versus PBS.

DISCUSSION

LPS are everywhere in the environment—from the food we eat to the air we breathe (24). LPS is known to elicit changes in mitochondrial physiology and several previous reports have explored the mitochondrial effects of LPS, though results are conflicted (25). Some report an increase in mitochondrial content and respiration (26), whereas others report a reduction
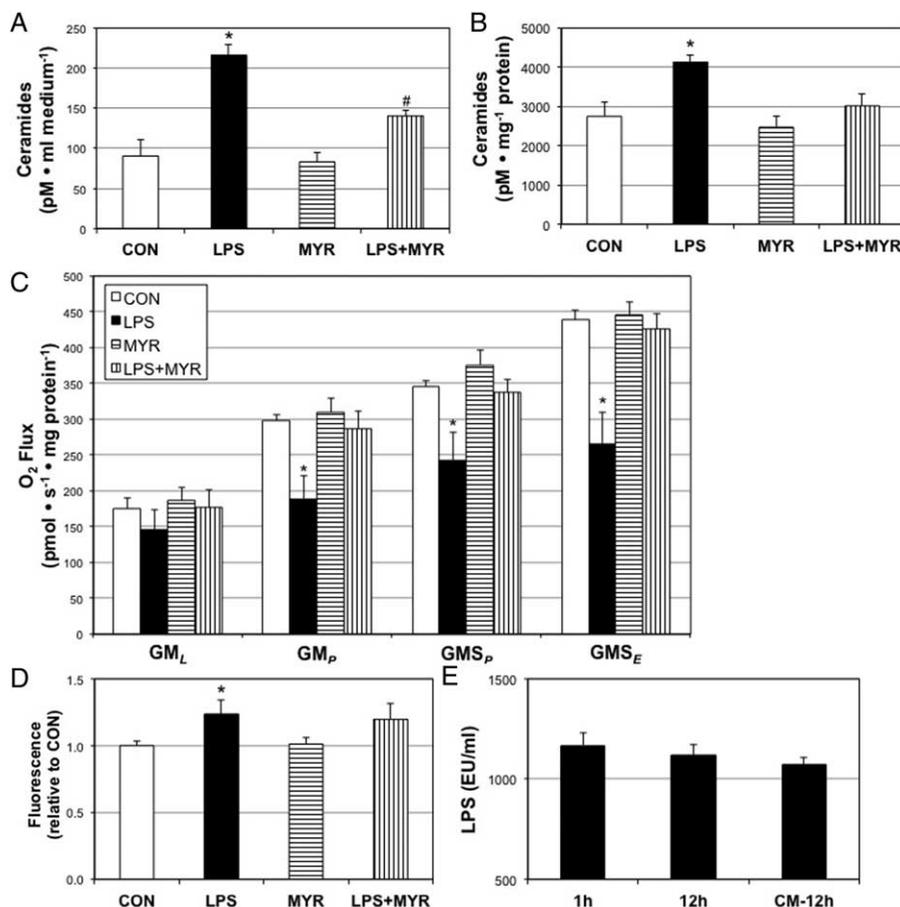

Fig. 6. **Conditioned medium from LPS-treated macrophages reduces myotube mitochondrial respiration, but not with ceramide inhibition.** RAW264.7 macrophages were treated with LPS (100 ng/mL) ± myriocin (10 μM) for 12 h. Ceramides were determined from macrophage-conditioned medium (A; n = 6). Macrophage-conditioned medium was transferred to C2C12 myotubes for 12 h (n = 5), after which myotube ceramides (B; n = 6) and respiration was analyzed (C; n = 6). DCF fluorescence was used to determine radical production (D; n = 3). LPS in culture medium did not change significantly after 1 or 12 h treatments on macrophages or following 12 h of incubation on myotubes with conditioned medium (CM-12 h) (E; n = 3). (See "Methods" for respiration protocol details.) $^*P < 0.05$ for treatment versus CON. #$P < 0.05$ for treatment versus all others.
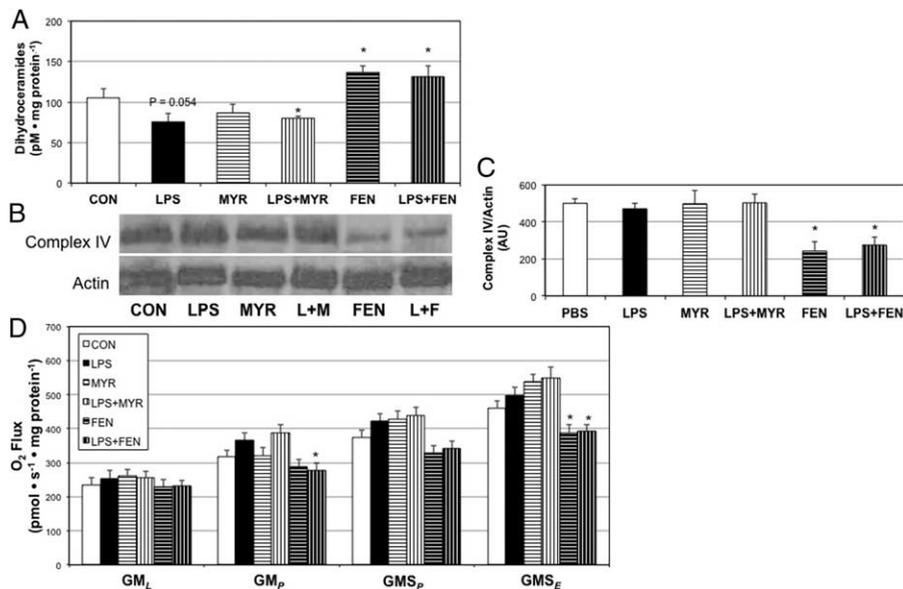
FIG. 7.   **Dihydroceramide desaturase inhibition reduces complex IV and reduces respiration.** C2C12 myotubes were treated with LPS (100 ng/mL), ± myriocin (MYR; 10 µM), or ± fenretinide (FEN; 5 µM) for 12 h. Following treatment, samples were analyzed for dihydroceramides (A; n = 6), complex IV protein (B and C; n = 6), and respiration (D; n = 6; see Fig. 2 legend for respiration details). $^*P < 0.05$ for treatment versus CON.

(27) with elevated LPS. Some of the incongruent findings regarding LPS and mitochondrial changes in previous reports may be due to disparate study conditions; study models exploring LPS-induced mitochondrial alterations range from isolated mitochondria to cell cultures to whole tissue following animal injections. Interestingly, our studies reveal conflicted results even within the same tissue/cell.

Combined with our previous observations revealing both LPS-induced sphingolipid accrual in muscle (11) and ceramide-mediated mitochondrial disruption in muscle (12–14, 22,28), we questioned whether the seemingly deleterious mitochondrial effects of LPS on skeletal muscle are dependent on altered ceramide metabolism. Although cultured myotubes experience a significant increase in mitochondrial respiration following LPS incubation (Fig. 2), muscle tissue from LPS-injected mice experienced reduced respiration (Fig. 4). We were able to reconcile these findings by using a macrophage-conditioned medium step before myotube treatment to more

closely mimic tissue milieu, i.e., heterogeneous cell populations (Fig. 7). In so doing, myotubes treated with the medium from LPS-treated macrophages experienced a reduction in mitochondrial respiration, similar to the whole muscle response with LPS injections. Ultimately, however, our data suggest Cer are not necessary for the decayed mitochondrial function with LPS, considering that Cer were increased with LPS treatment in both isolated muscle cell culture and whole muscle tissue. Nevertheless, the apparent protection provided by myriocin, a ceramide inhibitor, suggested that some component of sphingolipid metabolism is relevant. Indeed, upon further scrutiny, we found that DhCer accrue and accurately predict LPS-induced mitochondrial changes.

Siddique et al. (29) recently explored in depth the mitochondrial consequences of DhCer, revealing that DhCer accrual reduced mitochondrial respiration and appeared to selectively reduce complex IV expression. Our data corroborate these observations. We found that states of increased DhCer accrual, such as use of fenretinide, reduced mitochondrial respiration and complex IV protein levels. These findings are somewhat incongruous with our previous work, where we studied the mitochondrial effects of Cer and in so doing used short-chain DhCer as proof of concept that Cer were the relevant lipid (12). It is feasible that longer-chain species—those that accrue in biological conditions—are the significant DhCer mediators of LPS-induced mitochondrial alterations.

Several hemodynamic features of sepsis provide an enlightening context to our findings. In particular, reduced tissue perfusion is a primary pathological event in elevated LPS conditions (30,31), which makes the reduced mitochondrial oxygen consumption in muscle that we observed a logical outcome. A mechanism that may mediate this reduced perfusion/reduced respiration scenario is altered mitochondrial dynamics. We found that mitochondria tend to be smaller and experience greater fission with LPS treatments, which also

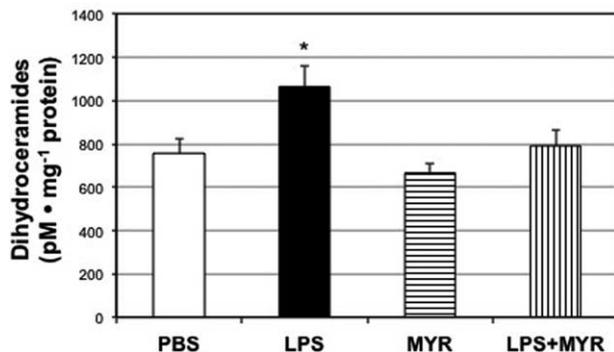FIG. 8.   **LPS injection increases dihydroceramides in soleus.** Adult male mice received IP injections of LPS (0.1 mg/kg body weight, daily) ± myriocin (0.3 mg/kg body weight, 3× per week) for 4 wk (n = 6). $^*P < 0.05$ for treatment versus PBS.

typifies mitochondrial morphology in low-flow, hypoxic states (32). This phenomenon (i.e., altered mitochondrial dynamics) may be relevant in reconciling the disparate mitochondrial effects of LPS over the years. We have previously found that induced mitochondrial fission tends to reduce mitochondrial oxygen consumption and increase ROS generation (12). However, many previous studies exploring the mitochondrial effects of LPS have measured mitochondrial function from isolated mitochondrial preparations (33), which obviously removes the mitochondria from the cell and, due to the lack of supporting and necessary structures, such as the endoplasmic reticulum (34), undoubtedly alters the structure of the organelle and, thus, potentially removes a pertinent part of LPS-induced mitochondrial changes.

Regardless of the tissue—liver or skeletal muscle—a primary player of the altered bioenergetics of a septic response in tissue, not to mention whole body, may be the macrophage. Among the various models used to study LPS-induced mitochondrial changes, it is important to note the situations in which a model is homogenous (i.e., not physiological) or heterogeneous (i.e., physiological). A noteworthy feature of C2C12 myotubes is the relative lack of CD14 expression compared with RAW264.7 macrophages, which may partly explain the unique response to LPS between the two cell types (35). CD14 is an important component of a cell recognizing and binding circulating LPS (36) and is likely at least partly relevant in LPS-related sphingolipid alterations (37).

The collective findings from this study are relevant in the case of low-level sepsis and mild infections, where deleterious mitochondrial changes can increase production of reactive oxygen species that compromise organ function (38,39), including skeletal muscle and liver (40). A review of the literature reveals that most previous efforts to understand the changes in mitochondrial physiology with septic conditions have studied the liver and hepatic mitochondria (33,41), with little attention on skeletal muscle. However, there is compelling cause to focus on skeletal muscle mitochondrial changes with LPS and sepsis considering the relative composition of the body (being roughly 40% muscle). Sepsis is associated with demonstrable whole-body metabolic changes. One such change is reduced metabolic rate (3), which may be a manifestation of our observation of reduced mitochondrial respiration within skeletal muscle in conditions of elevated LPS.

The aim of these studies was to determine the role of sphingolipids in LPS-induced mitochondrial alterations. Our results were somewhat inconclusive regarding the role of ceramide given our conflicting results from cell and tissue models, but the data corroborated previous evidence suggesting the importance of DhCer. Moreover, our results emphasize the importance of a heterogeneous cell population, especially the presence of the macrophage, in accurately reproducing the mitochondrial effects of LPS in skeletal muscle. Considering the prevalence of LPS in the environment and its role in human health (15,16), our findings suggest a benefit in exploring sphingolipid inhibition as a therapy to mitigate the deleterious consequences of mitochondrial alterations in tissues in states of elevated circulating LPS.

REFERENCES

1. Hotamisligil GS, Peraldi P, Budavari A, Ellis R, White MF, Spiegelman BM: IRS-1-mediated inhibition of insulin receptor tyrosine kinase activity in TNF-alpha- and obesity-induced insulin resistance. *Science* 271(5249):665–668, 1996.
2. Gregor MF, Hotamisligil GS: Inflammatory mechanisms in obesity. *Annu Rev Immunol* 29:415–445, 2011.
3. Kreymann G, Grosser S, Buggisch P, Gottschall C, Matthaei S, Greten H: Oxygen consumption and resting metabolic rate in sepsis, sepsis syndrome, and septic shock. *Crit Care Med* 21(7):1012–1019, 1993.
4. Kline JN, Cowden JD, Hunninghake GW, Schutte BC, Watt JL, Wohlford-Lenane CL, Powers LS, Jones MP, Schwartz DA: Variable airway responsiveness to inhaled lipopolysaccharide. *Am J Respir Crit Care Med* 160(1):297–303, 1999.
5. Yamamoto Y, Harashima A, Saito H, Tsuneyama K, Munesue S, Motoyoshi S, Han D, Watanabe T, Asano M, Takasawa S, et al.: Septic shock is associated with receptor for advanced glycation end products ligation of LPS. *J Immunol* 186(5):3248–3257, 2011.
6. Cani PD, Amar J, Iglesias MA, Poggi M, Knauf C, Bastelica D, Neyrinck AM, Fava F, Tuohy KM, Chabo C, et al.: Metabolic endotoxemia initiates obesity and insulin resistance. *Diabetes* 56(7):1761–1772, 2007.
7. Cani PD, Delzenne NM: The role of the gut microbiota in energy metabolism and metabolic disease. *Curr Pharm Des* 15(13):1546–1558, 2009.
8. Nelson MB, Swensen AC, Winden DR, Bodine JS, Bikman BT, Reynolds PR: Cardiomyocyte mitochondrial respiration is reduced by receptor for advanced glycation end-products (RAGE) signaling in a ceramide-dependent manner. *Am J Physiol Heart Circ Physiol* 309(1):H63–H69, 2015.
9. Opal SM, Scannon PJ, Vincent JL, White M, Carroll SF, Palardy JE, Parejo NA, Pribble JP, Lemke JH: Relationship between plasma levels of lipopolysaccharide (LPS) and LPS-binding protein in patients with severe sepsis and septic shock. *J Infect Dis* 180(5):1584–1589, 1999.
10. Ruiz AG, Casafont F, Crespo J, Cayon A, Mayorga M, Estebanez A, Fernadez-Escalante JC, Pons-Romero F: Lipopolysaccharide-binding protein plasma levels and liver TNF-alpha gene expression in obese patients: evidence for the potential role of endotoxin in the pathogenesis of non-alcoholic steatohepatitis. *Obes Surg* 17(10):1374–1380, 2007.
11. Holland WL, Bikman BT, Wang LP, Yuguang G, Sargent KM, Bulchand S, Knotts TA, Shui G, Clegg DJ, Wenk MR, et al.: Lipid-induced insulin resistance mediated by the proinflammatory receptor TLR4 requires saturated fatty acid-induced ceramide biosynthesis in mice. *J Clin Invest* 121(5):1858–1870, 2011.
12. Smith ME, Tippetts TS, Brassfield ES, Tucker BJ, Ockey A, Swensen AC, Anthonymuthu TS, Washburn TD, Kane DA, Prince JT, et al.: Mitochondrial fission mediates ceramide-induced metabolic disruption in skeletal muscle. *Biochem J* 456(3):427–439, 2013.
13. Bikman BT, Summers SA: Ceramides as modulators of cellular and whole-body metabolism. *J Clin Invest* 121(11):4222–4230, 2011.
14. Tippetts TS, Winden DR, Swensen AC, Nelson MB, Thatcher MO, Saito RR, Condie TB, Simmons KJ, Judd AM, Reynolds PR, et al.: Cigarette smoke increases cardiomyocyte ceramide accumulation and inhibits mitochondrial respiration. *BMC Cardiovasc Disord* 14:165, 2014.
15. Ng M, Fleming T, Robinson M, Thomson B, Graetz N, Margono C, Mullany EC, Biryukov S, Abbafati C, Abera SF, et al.: Global, regional, and national prevalence of overweight and obesity in children and adults during 1980–2013: a systematic analysis for the Global Burden of Disease Study 2013. *Lancet* 384(9945):766–781, 2014.
16. Kumar G, Kumar N, Taneja A, Kaleekal T, Tarima S, McGinley E, Jimenez E, Mohan A, Khan RA, Whittle J, et al.: Initiative in critical care outcomes research group of investigators: nationwide trends of severe sepsis in the 21st century (2000–2007). *Chest* 140(5):1223–1231, 2011.
17. Siddique MM, Bikman BT, Wang L, Ying L, Reinhardt E, Shui G, Wenk MR, Summers SA: Ablation of dihydroceramide desaturase confers resistance to etoposide-induced apoptosis in vitro. *PLoS One* 7(9):e44042, 2012.
18. Erickson KA, Smith ME, Anthonymuthu TS, Evanson MJ, Brassfield ES, Hodson AE, Bressler MA, Tucker BJ, Thatcher MO, Prince JT, et al.: AICAR inhibits ceramide biosynthesis in skeletal muscle. *Diabetol Metab Syndr* 4(1):45, 2012.
19. Pfaffl MW: A new mathematical model for relative quantification in real-time RT-PCR. *Nucleic Acids Res* 29(9):e45, 2001.
20. Bikman BT, Zheng D, Reed MA, Hickner RC, Houmard JA, Dohm GL: Lipid-induced insulin resistance is prevented in lean and obese myotubes by AICAR treatment. *Am J Physiol Regul Integr Comp Physiol* 298(6):R1692–R1699, 2010.

21. Layoun A, Samba M, Santos MM: Isolation of murine peritoneal macrophages to carry out gene expression analysis upon Toll-like receptors stimulation. *J Vis Exp* 98:e52749, 2015.

22. Thatcher MO, Tippetts TS, Nelson MB, Swensen AC, Winden DR, Hansen ME, Anderson MC, Johnson IE, Porter JP, Prince JT, et al.: Ceramides mediate cigarette smoke-induced metabolic disruption in mice. *Am J Physiol Endocrinol Metab* 307(10):E919–E927, 2014.

23. Suliman HB, Welty-Wolf KE, Carraway M, Tatro L, Piantadosi CA: Lipopolysaccharide induces oxidative cardiac mitochondrial damage and biogenesis. *Cardiovasc Res* 64(2):279–288, 2004.

24. Fageras Bottcher M, Hmani-Aifa M, Lindstrom A, Jenmalm MC, Mai XM, Nilsson L, Zdolsek HA, Bjorksten B, Soderkvist P, Vaarala O: A TLR4 polymorphism is associated with asthma and reduced lipopolysaccharide-induced interleukin-12(p70) responses in Swedish children. *J Allergy Clin Immunol* 114(3):561–567, 2004.

25. Levy RJ: Mitochondrial dysfunction, bioenergetic impairment, and metabolic down-regulation in sepsis. *Shock* 28(1):24–28, 2007.

26. Suliman HB, Carraway MS, Welty-Wolf KE, Whorton AR, Piantadosi CA: Lipopolysaccharide stimulates mitochondrial biogenesis via activation of nuclear respiratory factor-1. *J Biol Chem* 278(42):41510–41518, 2003.

27. Vanasco V, Magnani ND, Cimolai MC, Valdez LB, Evelson P, Boveris A, Alvarez S: Endotoxemia impairs heart mitochondrial function by decreasing electron transfer, ATP synthesis and ATP content without affecting membrane potential. *J Bioenerg Biomembr* 44(2):243–252, 2012.

28. Bikman BT: A role for sphingolipids in the pathophysiology of obesity-induced inflammation. *Cell Mol Life Sci* 69(13):2135–2146, 2012.

29. Siddique MM, Li Y, Wang L, Ching J, Mal M, Ilkayeva O, Wu YJ, Bay BH, Summers SA: Ablation of dihydroceramide desaturase 1, a therapeutic target for the treatment of metabolic diseases, simultaneously stimulates anabolic and catabolic signaling. *Mol Cell Biol* 33(11):2353–2369, 2013.

30. Trzeciak S, McCoy JV, Phillip Dellinger R, Arnold RC, Rizzuto M, Abate NL, Shapiro NI, Parrillo JE, Hollenberg SM, Microcirculatory Alterations in Resuscitation and Shock (MARS) investigators. Early increases in microcirculatory perfusion during protocol-directed resuscitation are associated with reduced multi-organ failure at 24 h in patients with sepsis. *Intensive Care Med* 34(12):2210–2217, 2008.

31. Derikx JP, Poeze M, van Bijnen AA, Buurman WA, Heineman E: Evidence for intestinal and liver epithelial cell injury in the early phase of sepsis. *Shock* 28(5):544–548, 2007.

32. Ong SB, Subrayan S, Lim SY, Yellon DM, Davidson SM, Hausenloy DJ: Inhibiting mitochondrial fission protects the heart against ischemia/reperfusion injury. *Circulation* 121(18):2012–2022, 2010.

33. Schumer W, Das Gupta TK, Moss GS, Nyhus LM, Erve PR: Effect of endotoxemia on liver cell mitochondria in man. *Z Exp Chir* 4(6):379–387, 1971.

34. Sebastian D, Hernandez-Alvarez MI, Segales J, Sorianello E, Munoz JP, Sala D, Waget A, Liesa M, Paz JC, Gopalacharyulu P, et al.: Mitofusin 2 (Mfn2) links mitochondrial and endoplasmic reticulum function with insulin signaling and is essential for normal glucose homeostasis. *Proc Natl Acad Sci U S A* 109(14):5523–5528, 2012.

35. Kawanishi N, Tanaka Y, Kato Y, Shiva D, Yano H: Lipopolysaccharide-induced monocyte chemotactic protein-1 is enhanced by suppression of nitric oxide production, which depends on poor CD14 expression on the surface of skeletal muscle. *Cell Biochem Funct* 26(4):486–492, 2008.

36. Triantafilou M, Triantafilou K: Lipopolysaccharide recognition: CD14, TLRs and the LPS-activation cluster. *Trends Immunol* 23(6):301–304, 2002.

37. Hanada K, Izawa K, Nishijima M, Akamatsu Y: Sphingolipid deficiency induces hypersensitivity of CD14, a glycosyl phosphatidylinositol-anchored protein, to phosphatidylinositol-specific phospholipase C. *J Biol Chem* 268(19):13820–13823, 1993.

38. Galley HF: Oxidative stress and mitochondrial dysfunction in sepsis. *Br J Anaesth* 107(1):57–64, 2011.

39. Sprong RC, Winkelhuyzen-Janssen AM, Aarsman CJ, van Oirschot JF, van der Bruggen T, van BS, Asbeck. Low-dose N-acetylcysteine protects rats against endotoxin-mediated oxidative stress, but high-dose increases mortality. *Am J Respir Crit Care Med* 157(4 pt 1):1283–1293, 1998.

40. Llesuy S, Evelson P, Gonzalez-Flecha B, Peralta J, Carreras MC, Poderoso JJ, Boveris A: Oxidative stress in muscle and liver of rats with septic syndrome. *Free Radic Biol Med* 16(4):445–451, 1994.

41. Lin HC, Liu SY, Lai HS, Lai IR: Isolated mitochondria infusion mitigates ischemia-reperfusion injury of the liver in rats. *Shock* 39(3):304–310, 2013.